



This is a repository copy of *Critical damage modes in high-performance drilling of carbon fibre reinforced epoxy composites*.

White Rose Research Online URL for this paper:  
<https://eprints.whiterose.ac.uk/id/eprint/225041/>

Version: Published Version

---

**Proceedings Paper:**

Kerrigan, K. [orcid.org/0000-0001-6048-9408](https://orcid.org/0000-0001-6048-9408), Phadnis, V.A., M'Saoubi, R. et al. (1 more author) (2025) Critical damage modes in high-performance drilling of carbon fibre reinforced epoxy composites. In: Dröder, K. and Hürkamp, A., (eds.) Procedia CIRP. 3rd CIRP Conference on Composite Material Parts Manufacturing (CCMPM2024), 25-27 Sep 2024, Braunschweig, Germany. Elsevier BV , pp. 100-106.

<https://doi.org/10.1016/j.procir.2024.11.003>

---

**Reuse**

This article is distributed under the terms of the Creative Commons Attribution-NonCommercial-NoDerivs (CC BY-NC-ND) licence. This licence only allows you to download this work and share it with others as long as you credit the authors, but you can't change the article in any way or use it commercially. More information and the full terms of the licence here: <https://creativecommons.org/licenses/>

**Takedown**

If you consider content in White Rose Research Online to be in breach of UK law, please notify us by emailing [eprints@whiterose.ac.uk](mailto:eprints@whiterose.ac.uk) including the URL of the record and the reason for the withdrawal request.



[eprints@whiterose.ac.uk](mailto:eprints@whiterose.ac.uk)  
<https://eprints.whiterose.ac.uk/>

3rd CIRP Conference on Composite Material Parts Manufacturing

# Critical damage modes in high-performance drilling of carbon fibre reinforced epoxy composites

Kevin Kerrigan<sup>a,\*</sup>, Vaibhav A. Phadnis<sup>a</sup>, Rachid M'Saoubi<sup>b</sup>, Richard J. Scaife<sup>a</sup><sup>a</sup>Advanced Manufacturing Research Centre, University of Sheffield, Advanced Manufacturing Park, Wallis Way, S60 5TZ, Rotherham, UK<sup>b</sup>Materials and Technology Development Processes, Seco Tools AB, Fagersta, SE-73782, Sweden\* Corresponding author. Tel.: +44-114-222-9588 ; E-mail address: [k.kerrigan@amrc.co.uk](mailto:k.kerrigan@amrc.co.uk)

## Abstract

The growing number of fibre deposition methods for composite structure enables highly tailored, high-performance architectures from one design intent to another. This raises the question, “How much should damage tolerances differ for one composite part design to another?” This initiates a framework for further exploration of the boundaries of acceptability, using a quantitative approach to assess the influence of process parameters on in-service performance. The framework is illustrated through a case study of a feature machined into a composite structure, namely a hole for part assembly. Mechanical and thermal hole defects were deliberately induced during dry drilling of quasi-isotropic pre-impregnated laminates. In-process forces and temperatures in combination with post-machining microscopy, X-ray computed tomography and scanning electron microscopy revealed micro-damage leading to isolated, global defects of delamination and thermal damage types. Comparisons with healthy, undamaged holes in static mechanical tests enabled quantitative assessment of the impact of different damage types on in-service performance, in this case compressive strength, of a composite part. High-speed drilling (52% faster) reduced strength (3.5%) due to hole geometry errors. Low-speed drilling (11.5x slower) increased strength (2%). Delamination (40% faster) reduced strength (2.5%). Future research should focus on defect implications, virtual defects and testing thereof, and in-situ monitoring.

© 2024 The Authors. Published by Elsevier B.V.

This is an open access article under the CC BY-NC-ND license (<http://creativecommons.org/licenses/by-nc-nd/4.0/>)

Peer-review under responsibility of the scientific committee of the 3rd CIRP Conference on Composite Material Parts Manufacturing.

**Keywords:** CFRP; Carbon-Epoxy; composites; thermal damage; drilling; delamination; open-hole compression

## 1. Introduction

The aerospace market is currently experiencing (a) Growing order books in 2024 - 2043 forecast of The Boeing Company and Airbus [1, 2], requiring higher rates of production of more sustainable replacement single-aisle, widebody and freight aircraft designs; (b) Novel aircraft designs, such as electric vertical take-off and landing (eVTOL) aircraft, being released from 2024 onwards [3]; (c) Increasing sustainability requirements [4] spanning both aircraft design and production. To address these challenges, aerospace manufacturers are turning to superior strength-to-weight and stiffness-to-weight ratios of lightweight high-performing materials, particularly fibre reinforced polymer (FRP) composites to achieve sustainable solutions for aerospace designs [5]. Composites offer tailored material properties and localised optimisation, making them ideal for applications requiring high strength-to-weight and stiffness-to-weight ratios. However, manufacturing quality assessment, derived from damage tolerances applied to composite parts [6],

remain critical concerns, especially when considering the potential impact on in-service performance. This research builds upon previous CIRP working group findings [7] and presents a framework for evaluating the influence of different manufacturing defects on the performance of composite parts. Specifically, focus is placed on the case of hole drilling in a carbon fibre reinforced polymer (CFRP) structure. High-speed machining, a common practice in the aerospace industry, can exacerbate damage modes such as surface finish, delamination, fibre pull-out, and resin thermal degradation [8, 9, 10]. These defects can significantly affect part quality and in-service mechanical performance [11, 12]. Approaching this challenge, a method is suggested for manufacturers to explore the damage domain of a part, establish potentially critical defect types, isolate them and quantify defect criticality through mechanical testing. This case study investigates the impact of various drilling process parameters on damage formation and subsequent part performance. The relative criticality of delamination and resin thermal degradation are considered in this investigation, with deliberate setups and cutting parameters used to isolate each specific

2212-8271 © 2024 The Authors. Published by Elsevier B.V.

This is an open access article under the CC BY-NC-ND license (<http://creativecommons.org/licenses/by-nc-nd/4.0/>)

Peer-review under responsibility of the scientific committee of the 3rd CIRP Conference on Composite Material Parts Manufacturing.

Table 1. Test matrix for parametric drilling trials to cutting parameters to isolate the causes of mechanical and thermal damage.

Desired hole condition	Cutting parameters			
Intended healthy holes	Feed (f, mm/rev)	0.03	0.04	0.05
	Spindle speed (n, rpm)	3000	4000	5000
Holes with intended delamination	Feed (f, mm/rev)	0.05	0.1	0.2
	Spindle speed (n, rpm)	3000	4000	5000
Holes with excessive process heat	Case 1: short drill-workpiece contact			
	Feed (f, mm/rev)	0.02	0.035	0.05
	Spindle speed (n, rpm)	10000	12000	15000
	Case 2: extended drill-workpiece contact			
	Feed (f, mm/rev)	0.013	0.014	0.015
	Spindle speed (n, rpm)	8300	8900	9600

defect. Process mapping tools, applied as part of this methodology, have been shown to aid in understanding the effects of cutting parameters on machined composite quality [13]. This case study focuses on dry drilling of aerospace-grade CFRP laminates and investigates the effects of high feed rates, high spindle speeds, and tool wear. Thermal energy exposure of the workpiece, relative to its polymer glass-transition temperature ( $T_g$ ), is assessed by measuring workpiece maximum temperature using infrared thermography. Chip morphology is analysed using scanning electron microscopy (SEM) to understand the mechanistic differences in material removal above and below the  $T_g$ . Finally, these are used to evaluate the impact of critical damage modes on residual strength through open-hole compression (OHC) tests.

## 2. Methodology

Drilling trials were conducted to analyse material removal in cured CFRPs using cutting conditions leading to either of the concerned defects/damage modes, i.e. delamination and resin thermal degradation. To facilitate this, abusive drilling parameters (high feed rates, high cutting speed and worn drills) were deliberately used. Delamination was ensured by forcing high axial feeds, while resin thermal degradation was forced using two strategies described in Table 1).

In the first strategy, low axial feeds (f) were combined with moderate spindle speeds (n). This resulted in extended drill-workpiece contact causing excessive rubbing and prolonged heat at their interface. In the second strategy, high spindle speeds were combined with moderate feeds, leading to shorter drill exposure times and more opportunity to rub. In both strategies feed and speed combinations ensured the same exposure time for the comparison purpose. The most appropriate cutting parameters allowing healthy holes, as well as those giving rise to aforementioned critical damage modes/defects were short-listed from above exercise to generate OHC test samples. These are listed in 2.

## 3. Drilling of CFRP

### 3.1. Workpiece material specification

Quasi-isotropic carbon/epoxy plates were manufactured from unidirectional (UD) 5320-1/T650 prepreg (ply thickness

Table 2. Cutting parameters used to drill OHC coupons with healthy, delaminated and thermally damaged holes.

Intended hole type (Batch of 8)	Feed (f, mm/rev)	Spindle speed (n, rpm)	Drill condition	Backing plate
Batch A - Healthy	0.05	5000	New	Yes
Batch B - Healthy	0.05	5000	Worn	Yes
Batch C - Delam.	0.2	3000	New	No
Batch D - Delam.	0.2	3000	Worn	No
Batch E - Heat exposure: Case 1	0.05	15000	New	Yes
Batch F - Heat exposure: Case 1	0.05	15000	Worn	Yes
Batch G - Heat exposure: Case 2	0.013	9600	New	Yes
Batch H - Heat exposure: Case 2	0.013	9600	Worn	Yes

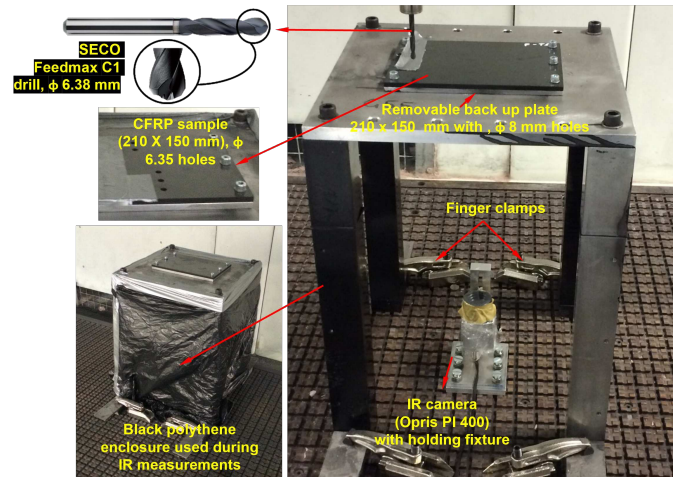


Fig. 1. Experimental setup for CFRP drilling trials (a) force measurement (b) temperature measurement.

0.14 mm). Woven fabric variant (ply thickness 0.19 mm) of the same material was used to form the top- and bottom-most plies of the laminate. The proposed layup was vacuum-bagged, debulked in an oven using atmospheric pressure (101 kPa), and cured using manufacturer data sheet cure cycle B - low temperature 121 °C initial cure followed by a free-standing post-cure to 177 °C [14]. This resulted in a cured laminate with fibre volume fraction ( $V_f$ ) of 58% and nominal thickness of  $6.06 \pm 0.02$  mm; cured ply sequence was [(W[0/90])(((0°/45°/90°/-45°)5)s)(W[90/0])]. CFRP panels (600 x 600 x 6 mm) were then cut in two smaller (150 x 90 mm) and (210 x 150 mm) sizes to suit the relevant fixtures while drilling (refer to Figure 2a and 2b). Glass-transition temperature ( $T_g$ ) of cured laminate was determined using dynamic mechanical analysis (DMA) test confirming to ASTM standard D7028-07(2015) as per Figure 2, which enabled the usable process-heat range for the workpiece to be identified.

### 3.2. Drilling experiments

Dry drilling trials were conducted using CMS Ares 5-axis CNC machining centre (max. spindle power - 14 kW, max. spindle speed - 24,000 rpm and max. feed rate - 30 m/min) with a Fanuc 30i NC controller to generate a industrially relevant, repeatable, accurate parametric experiment. As per Figure 1, the fixture used for thermal damage experiments was fabricated to enable workpiece exit temperature measurement. External air supply was used to cool down and clear-off accumulated CFRP chip during machining. Both new and worn geometries of the

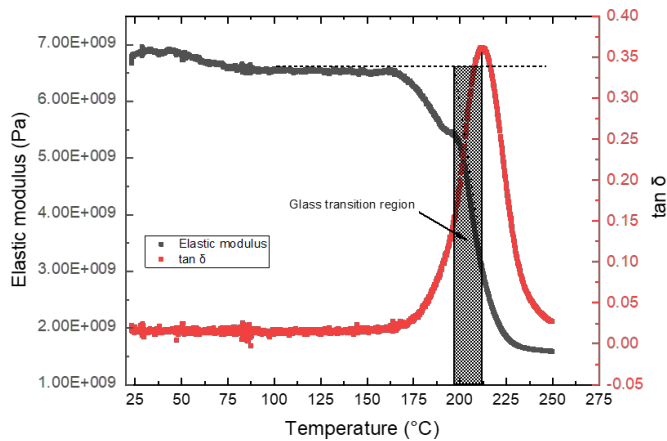


Fig. 2. DMA analysis and glass transition temperature of 5320-1/T650 composite

Seco C1-Feedmax drills, having a helix angle of  $30^\circ$ , Point angle – Primary  $130^\circ$ , Secondary  $60^\circ$ ; Dc tolerance – m7; Chamfer angle –  $100^\circ$ ; Shank – h6 were used. Worn cutting edges were purposefully chipped using a controlled grinding process to mimic condition at the end of drill life. A measurable portion of CVD coating loss occur. All new and worn drill geometries were measured for cutting edge rounding (CER)[15] using Alicona InfiniteFocus G5 optical microscope. This analysis indicated that new drills achieved a  $\Delta R$  value in the range of 24 to 29  $\mu\text{m}$ , whilst worn drills were in the range of 70 to 80  $\mu\text{m}$ . Edge radius values were in the range 21 - 26  $\mu\text{m}$  and 20 - 30  $\mu\text{m}$  respectively. This result indicated that whilst the grinding process chipped away the diamond coating, it left the carbide substrate geometry relatively sharp. The equivalent flank wear value measured via optical microscope was approximately 60  $\mu\text{m}$ .

Each drill was used to make no more than 20 holes to minimise the effect of tool wear. Delamination at drill-entry and -exit was measured using an Olympus GZX 12 optical microscope. Cutting forces were recorded using an 8-channel Kistler dynamometer, type 9129A, on a similar fixture. Cutting temperature on the drill-exit side of the workpiece was measured using an Optris PI400 thermal imaging camera (calibrated temperature range – 0 to 250  $^\circ\text{C}$ , frame rate – 80 Hz, optical resolution – 382 x 288 pixels). Drill-exit side of CFRP workpiece was painted with high-emissivity black paint of 0.95 emissivity. The temperature fixture, shown in Figure 1b, was enclosed using black polythene to restrict radiation entering from external sources. The backing plate was integrated in both fixtures to minimise delamination and removed during delamination-specific defect generation. Hole quality was assessed using Nikon Evolution CMM with Renishaw SP25-1/stylus: 3x30 scanning probe. SEM scans of drills, borehole surface and CFRP chip were obtained using Carl Zeiss variable pressure EVO LS25 microscope to comprehend post-machining changes in their microstructures along with a Nikon XTH-225 x-ray microCT machine using a voltage and current of 175 kV and 143  $\mu\text{A}$ , respectively and a 0.25 mm Copper filter to generate 3142 projections followed by post processing in CT Pro 3D v3.1 by Nikon.

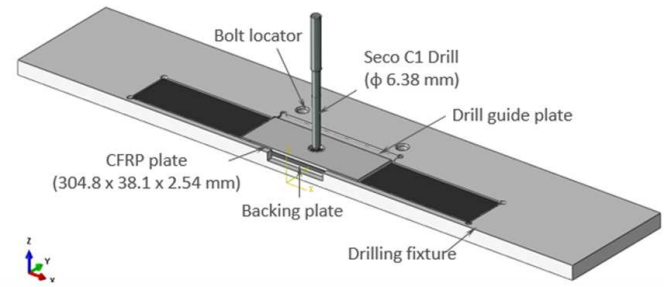


Fig. 3. Schematic of drilling fixture for preparation of OHC specimens.

## 4. Structural testing

### 4.1. Sample preparation

A bespoke fixture, shown in Figure 3, was manufactured for compression testing. It consists of three main parts – a rectangular plate with a slot to accommodate CFRP OHC specimen, a backing plate and a drill guiding plate. A backing plate was used to avoid delamination at the drill-exit side of CFRP specimen when thermal damage was intended. It was removed when delamination was intended. Bolt locators on the fixture plate were used to clamp the fixture to the machine bed, vacuum pressure provided additional fixing support. A drill guiding plate allowed consistency and accuracy in locating the centre of the CFRP coupon.

### 4.2. Open-hole compression (OHC) testing

40 open-hole CFRP samples (average dimensions of 304.8 x 31.8 x 2.6 mm in accordance with ASTM D6484/6484M [16]) categorised in 8 batches of 5 samples each were tested under uniaxial compression load until failure. An industrial OHC fixture was used to facilitate these tests as shown in Figure 4a. The fixture had anti-buckling guides to prevent out-of-plane bending (buckling) of tested specimens. A uniaxial compression test of a balanced, symmetric laminate was performed with a centrally located hole. Ultimate strength was calculated based on the net cross-sectional area, disregarding the presence of the hole. While the hole causes a stress concentration and reduced net section, it is a common aerospace practice to develop notched design allowable strengths based on gross section stress to account for various stress concentrations, e.g. fastener holes, free edges, flaws, damage, and so forth, not explicitly accounted for in stress calculation [16]. The test specimen, shown in Figure 4c was face-supported in a multi-piece bolted support fixture. Two acceptable test procedures are provided in [16]. An Instron testing machine with maximum loading capacity of 100 kN was used. A typical test result is shown in Figure 4b. Figure 4c clearly shows that the specimen failed exactly at the hole's location and the dominating failure resulted from axial splits in  $0^\circ$  and  $45^\circ$  plies. The end-loaded data typically display initial nonlinear behaviour at low force levels due to seating of the specimen/fixture assembly underneath the load platens, but then exhibit linear behaviour to failure as observed in the force-displacement plot shown in Figure 4b). The tests were re-

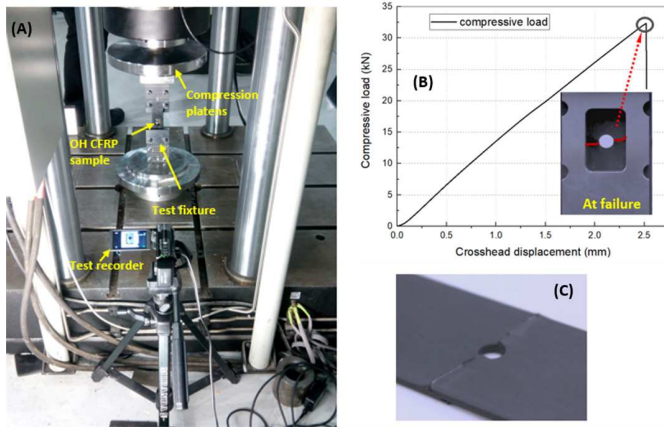


Fig. 4. (a) Open-hole compression test setup [6]; (b) a typical open-hole compression test response; (c) a typically cracked CFRP specimen under uni-axial compressive loading.

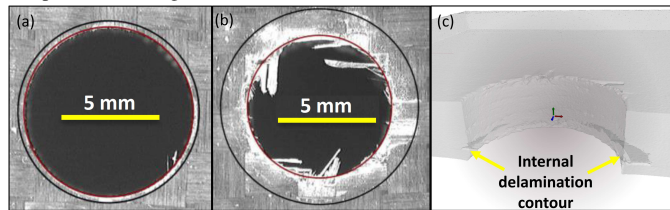


Fig. 5. Hole quality using delamination factor metric showing hole exit generated using (a) healthy parameters (Batch A), (b) delamination parameters (Batch D), with (c) microCT scan image indicating internal delamination.

peated for all sample batches considered in this study and the compressive strength calculated based on the maximum compressive load carried by a sample and its gross cross-section area in the absence of a circular notch.

## 5. Results and discussion

### 5.1. Assessment of hole geometry and delamination

The geometries achieved for all holes were repeatable and within the range of  $6.35 \text{ mm} \pm 25 \mu\text{m}$  for diameter, apart from the high-speed holes generated using thermal case 1 parameters, which were oversized by approximately 0.2 to 0.4 mm. Holes were often narrowly undersized due to impact force and worn drills, but oversized with high spindle speed. Drill condition and axial feed marginally impacted hole size though more severe impact was noted to circularity, with errors of upwards of  $200 \mu\text{m}$  observed in batches D, E, F and G.

Drilling induced delamination in composites is directly related to thrust force exerted by the drill [8, 17]. Highly localised compressive forces resulted from drill-entry, and tensile forces from drill-exit could result in large interlaminar shear stresses leading to loss of adhesive bonding between neighbouring plies. A maximum thrust force of 760 N was reported using a worn drill ( $f = 0.2 \text{ mm/rev}$ ,  $n = 3000 \text{ rpm}$ ,  $\Delta r 80 - 90 \mu\text{m}$ ). Delamination was assessed using the industrially relevant delamination factor ( $F_d$ ), the ratio of maximum delamination diameter ( $D_{max}$ ) to drill nominal diameter ( $D_h$ ). Figure 5 shows the effect of increasing the axial feed on drill-exit delamination. As a general trend, thrust forces increased linearly with axial

feeds for low and moderate spindle speeds (from 3000 to 8300 rpm), yet reduced for high spindle speeds, for  $8300 \text{ rpm} < n < 10000 \text{ rpm}$ , before reaching a plateau in the case of higher spindle speeds  $> 10000 \text{ rpm}$ . For the high feed and low-to-moderate spindle speed scenario, the drill's static inertia potentially overcomes its rotary inertia resulting in a punching action. On the contrary, with high spindle speeds, the drill's rotary inertia, in combination with matrix-softening from the elevated temperatures, appears to ensure delamination-free penetration of the workpiece. This suggests benefits for the use of high-feed, high-speed drilling of composites, though previous researchers have found deleterious effects of high cutting temperatures on the integrity of epoxy resin [10].

### 5.2. Cutting temperature of CFRP workpiece

Workpiece temperature ( $T_w$ ) was measured at hole exit just after drill shoulder break-out with the average of five measurements reported. The effect of increase in spindle speed using recommended axial feed ( $0.03 \text{ mm/rev}$ ), and increase of axial feed at constant spindle speed ( $5000 \text{ rpm}$ ) on the workpiece temperature for new and worn drills is plotted in Figures 6a-b. It was noted that temperature rise in workpiece was highly non-linear for both drill geometries as spindle speed increased from  $3000 \text{ rpm}$  to  $15000 \text{ rpm}$  (refer to Figure 6a). For pristine drills, the rate of temperature rise was much lower compared to that of worn drill, and the highest temperature remained within the glass transition range. As a result, resin smearing on the CFRP borehole surface was quite evident though matrix burnout was not observed. In the case of the worn drill, owing to constantly altering cutting edge geometry, workpiece temperature rise was non-uniform though kept increasing with steep slope in most instances. The highest temperature was noted to exceed  $T_g$ , and resulted in matrix burnout forming pits on the borehole surface. Adverse to the effect of increase of spindle speeds, workpiece temperature decreased almost linearly for both pristine and worn drill geometries when axial feed increased from  $0.02 \text{ mm/rev}$  to  $0.2 \text{ mm/rev}$  at constant spindle speed of  $5000 \text{ rpm}$  (refer to Figure 6b). At low axial feed ( $f = 0.02 \text{ mm/rev}$ ), workpiece temperature was as high as  $176$  and  $198 \text{ }^\circ\text{C}$  using new and worn-drills, respectively. This could be due to the prolonged drill-workpiece contact resulting in extensive rubbing. As feed was increased further, drill-workpiece exposure time reduced continuously, and cutting temperature almost linearly. The workpiece temperature was observed to be below  $T_g$  for most instances. The measurement of drill-side temperature was not a focus of this study, though scholarly information regarding this could be found in the literature [2,5,12]. From [5], it is interesting to note that drill's temperature increased constantly with increase in axial feed, analytical models predicted the tool temperature to be as high as  $290 \text{ }^\circ\text{C}$  for spindle speed of  $8500 \text{ rpm}$  and axial feed of  $0.2 \text{ mm/rev}$  supporting the case of matrix softening. Post-machining SEM scans of drills showed particular wear patterns characteristic of high spindle speed and high axial feed scenarios (refer to Figures 7a-b). In case of former, it was observed that drill wear primarily concentrated at cutting edges (Figure 7a showing wear of cutting edge-1 on edge-

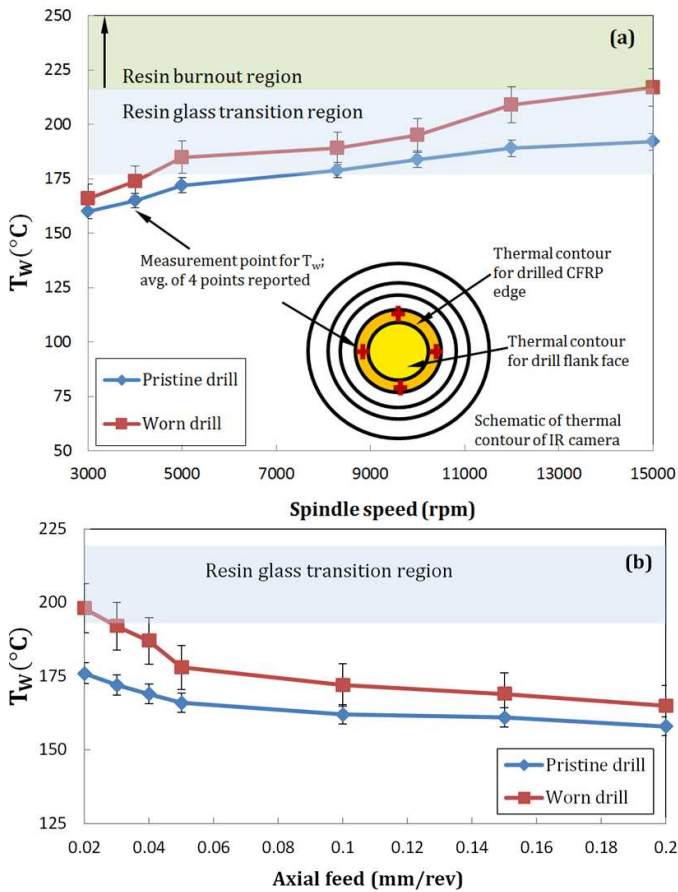


Fig. 6. Effect of (a) spindle speed (constant axial feed: 0.03 mm/rev); and (b) axial feed (constant spindle speed: 5000 rpm) on workpiece cutting temperature by drill wear.

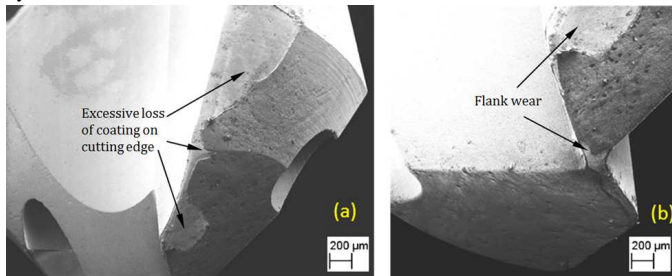


Fig. 7. Typical tool wear patterns in CFRP drilling: effect of high spindle speed and low feed ( $f = 0.03$  mm/rev,  $n = 15000$  rpm) (b) effect of high feed and low spindle speed ( $f = 0.1$  mm/rev,  $n = 3000$  rpm)

prepared C1 drill after 40 holes). A significant portion of coating flaked-off the surface exposing WC substrate. In latter case (Figure 7b showing wear of flank area of edge prepared C1 drill after 40 holes), drill wear mostly concentrated at the flank area, though its severity was lesser.

### 5.3. Chip morphology and mechanism of material removal

Effect of cutting temperatures on CFRP chip morphology was assessed using SEM scans of borehole surfaces. Using very low feed ( $f : 0.012$ - $0.015$  mm/rev), recommended spindle speed ( $n = 5000$  rpm) and a pristine drill yielded a distinct case where metal-like surface finish on CFRP borehole surface was observed with  $R_a$  as low as  $0.7 \mu\text{m}$ , in the best case. This was

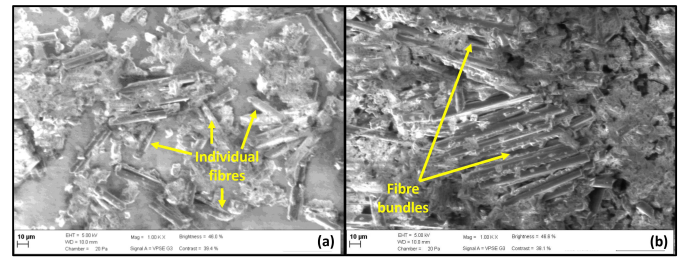


Fig. 8. CFRP Chip morphology : (a) just below  $T_g$  ( $n = 8300$  rpm) and (b) above  $T_g$  ( $n = 10000$  rpm),  $f = 0.03$  mm/rev and using new drill.

speculated to be due to excessive rubbing at the drill-workpiece interface resulting in the overlap of  $T_w$  and  $T_g$  regions (similar to the region coloured in light purple, Figures 6a-b). Viscous epoxy matrix appeared to coat the borehole surface uniformly; the apparent roughness of which was measured using a stylus profilometer reflecting in the measured  $R_a$  value. Minimal pitting towards drill-exit side was also noticed, though attributed to the resin-rich area/dry spots from the natal phase.

Use of higher spindle speeds ( $n > 8000$  rpm) showed discrete material removal mechanisms: two cases, when  $T_w$  was just above and just below  $T_g$ , were considered. For  $T_w$  just below  $T_g$ , carbon-fibres fractured virtually discretely as per Figure 8a, owing to fully-intact resin and strong fibre-matrix bonding. For the case of  $T_w > T_g$ , shown in Figure 8b, fibres were cut in bundles owing to thermally softened epoxy matrix. This could potentially lead to multiple crack initiation points in drilled structures, affect surface roughness and compromise the structural integrity. To further understand this, the worst-case scenario was considered; CFRP laminate drilled using a worn drill with recommended feed ( $f = 0.05$  mm/rev) and high spindle speed ( $n = 15000$  rpm). From microscopy analysis, resin smearing as well as pitting from matrix burnout was evident, as depicted in Figure 9 at both drill entry and exit sides of drilled surface. Higher resolution SEM images of these macro-damage mechanisms revealed their link with discrete micro-level defects such as uncut fibres, fibre-matrix de-bonds and fibre pull-out. The effect of tool edge rounding was potentially seen via the presence of shear marks on the cut surface indicating fibre ploughing in the absence of a sharp cutting edge.

### 5.4. Open-hole compression strength

A boxplot summary of OHC strengths is shown in Figure 10 for all CFRP samples, as described in Table 2. The scatter of strengths is greater for the holes drilled using worn drills. Batches A (new) and B (worn) used healthy parameters. Considering the mean strength results, OHC strength of 316 MPa was reported for batch A which reduced by 0.64% for batch B. For batches C and D with intended delamination using new and worn drills, magnitudes of OHC strengths were 2-2.7% lower than the average baseline and no significant drop observed for sample drilled using a worn drill when compared to new drill. The standard deviation across all batches was comparable, though future work should look to minimise variation. Batch F represented the worst case scenario of all mean OHC strengths, with average strength 3.5% lower than the baseline.

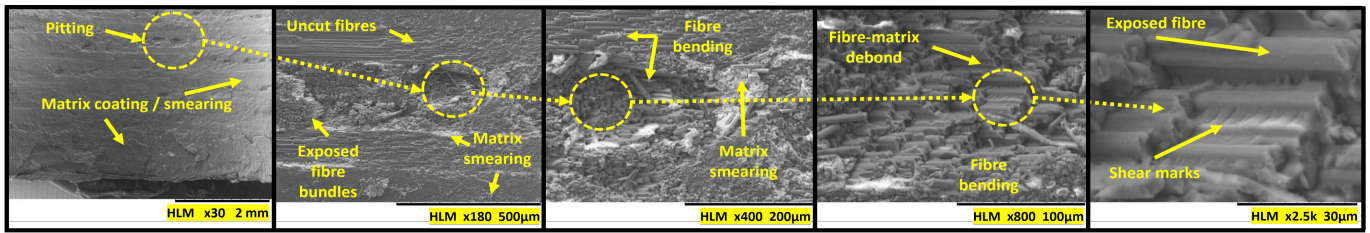


Fig. 9. Electron microscopy scan of CFRP borehole surface showing progressive zooms of thermal damaged: Case 1 defects generated ( $f = 0.05$  mm/rev,  $n = 15000$  rpm, worn drill).

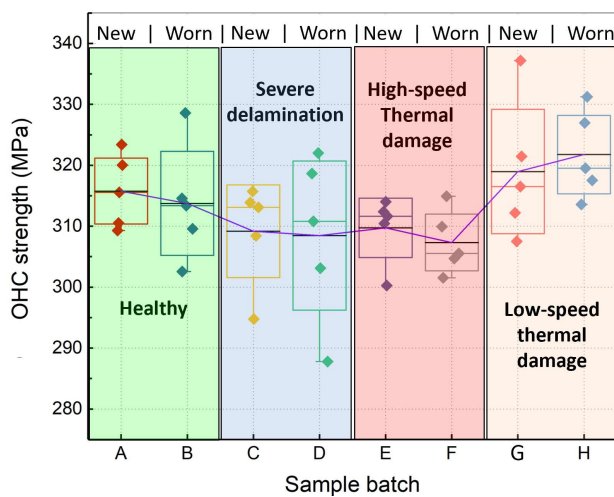


Fig. 10. OHC strength of drilled CFRP samples. Note: For comprehension of cutting parameters used to drill specimen batches A to H shown in above graph, please refer to 2.

On the other hand, the sample batches G and H exhibited higher strengths than the baseline – a maximum mean increase of 1-2% was reported, potentially due to low carbide edge radius.

## 6. Conclusions and future works

Delamination and thermal degradation of carbon fibre reinforced epoxy laminate were studied using dry, air blasted drilling conditions. SEM analysis revealed that micro-damage modes could lead to formation of cracks affecting the hole quality. Good quality holes were produced by selecting cutting parameters such that workpiece temperature remains just below its  $T_g$  and thrust forces below the threshold. In this case, optimal cutting conditions were identified as  $f = 0.05$  mm/rev and  $n = 5000$  rpm. Compressive strength of CFRP OHC samples drilled using high spindle speeds and industry-wide feed rates (samples E & F) was 3.5% lower than baseline OHC strength and 52% faster. Conversely, CFRP OHC samples drilled using very low axial feeds and cutting speeds (samples G & H) had 2% higher compressive strength than baseline but took 11.5 times longer. Samples with delamination were generated 40% faster, but showed a decrease of 2.5% in their OHC strengths compared to the baseline. Under compressive failure conditions, delamination demonstrated a similar level of criticality as it resulted in a 2.5% decrease in static compressive strength. Future works should consider the implications of such defects on

fatigue life of composite parts to fully determine their significance; virtual defect generation and testing; and in-situ defect monitoring techniques for early defect identification.

## Acknowledgements

The authors thank Mr. Jeffrey L. Lantrip, The Boeing Company, for insights and the AMRC membership for financial and technical support. AMRC technical staff are also acknowledged for expertise and support.

## References

- [1] Boeing, [Commercial market outlook](https://cmo.boeing.com/) (2024). URL <https://cmo.boeing.com/>
- [2] Airbus, [Global market forecast](https://www.airbus.com/en/products-services/commercial-aircraft/market/global-market-forecast) (2024). URL <https://www.airbus.com/en/products-services/commercial-aircraft/market/global-market-forecast>
- [3] J. Coykendall, M. Metcalfe, A. Hussain, T. Dronamraju, *Disrupting the future of mobility, Market analysis* (2022).
- [4] E. Commission, D.-G. f. Mobility, Transport, D.-G. f. Research, Innovation, Flightpath 2050 – Europe’s vision for aviation – Maintaining global leadership and serving society’s needs, Publications Office, 2011. doi:[10.2777/50266](https://doi.org/10.2777/50266).
- [5] A. André, M. Juntikka, C. Mattsson, T. Hammar, R. Haghani, *Sustainable repurpose of end-of-life fiber reinforced polymer composites: A new circular pedestrian bridge concept*, *Journal of Environmental Management* 367 (2024) 122015. doi:<https://doi.org/10.1016/j.jenvman.2024.122015>. URL <https://www.sciencedirect.com/science/article/pii/S0301479724020012>
- [6] M. R. Woodward, R. Stover, *Damage Tolerance*, Vol. 21, ASM International, 2001, pp. 295–301. doi:[10.31399/asm.hb.v21.a0003386](https://doi.org/10.31399/asm.hb.v21.a0003386). URL <https://doi.org/10.31399/asm.hb.v21.a0003386>
- [7] I. S. Jawahir, E. Brinksmeier, R. M’Saoubi, D. K. Aspinwall, J. C. Outeiro, D. Meyer, D. Umbrello, A. D. Jayal, *Surface integrity in material removal processes: Recent advances*, *CIRP Annals* 60 (2) (2011) 603–626. doi:<https://doi.org/10.1016/j.cirp.2011.05.002>. URL <https://www.sciencedirect.com/science/article/pii/S0007850611002046>
- [8] R. Teti, *Machining of composite materials*, *CIRP Annals* 51 (2) (2002) 611–634. doi:[https://doi.org/10.1016/S0007-8506\(07\)61703-X](https://doi.org/10.1016/S0007-8506(07)61703-X). URL <https://www.sciencedirect.com/science/article/pii/S000785060761703X>
- [9] R. Higuchi, S. Warabi, W. Ishibashi, T. Okabe, *Experimental and numerical investigations on push-out delamination in drilling of composite laminates*, *Composites Science and Technology* 198 (2020) 108238. doi:<https://doi.org/10.1016/j.compscitech.2020.108238>. URL <https://www.sciencedirect.com/science/article/pii/S0266353820303869>
- [10] K. Kerrigan, G. E. O’Donnell, *On the relationship between cutting temperature and workpiece polymer degradation during cfrp edge trimming*, *Procedia CIRP* 55 (2016) 170–175. doi:<https://doi.org/10.1016/j.procir.2016.03.030>

[//doi.org/10.1016/j.procir.2016.08.041](https://doi.org/10.1016/j.procir.2016.08.041).

URL <https://www.sciencedirect.com/science/article/pii/S2212827116309301>

- [11] E. Brinksmeier, S. Fangmann, R. Rentsch, [Drilling of composites and resulting surface integrity](#), *CIRP Annals* 60 (1) (2011) 57–60. doi:<https://doi.org/10.1016/j.cirp.2011.03.077>. URL <https://www.sciencedirect.com/science/article/pii/S0007850611000783>
- [12] S. Ashworth, J. P. A. Fairclough, J. Meredith, Y. Takikawa, K. Kerrigan, [Effects of tool coating and tool wear on the surface quality and flexural strength of slotted cfrp](#), *Wear* 498–499 (2022) 204340. doi:<https://doi.org/10.1016/j.wear.2022.204340>. URL <https://www.sciencedirect.com/science/article/pii/S0043164822001053>
- [13] M. J. Li, S. L. Soo, D. K. Aspinwall, D. Pearson, W. Leahy, [Influence of lay-up configuration and feed rate on surface integrity when drilling carbon fibre reinforced plastic \(cfrp\) composites](#), *Procedia CIRP* 13 (2014) 399–404. doi:<https://doi.org/10.1016/j.procir.2014.04.068>. URL <https://www.sciencedirect.com/science/article/pii/S2212827114000699>
- [14] Cytec, [Cycom® 5320-1 epoxy resin system \(01/06/2024 2015\)](#). URL [https://cstjmateriauxcomposites.wordpress.com/wp-content/uploads/2017/11/cycom5320\\_8hs.pdf](https://cstjmateriauxcomposites.wordpress.com/wp-content/uploads/2017/11/cycom5320_8hs.pdf)
- [15] A. Faraz, D. Biermann, K. Weinert, [Cutting edge rounding: An innovative tool wear criterion in drilling cfrp composite laminates](#), *International Journal of Machine Tools and Manufacture* 49 (15) (2009) 1185–1196. doi:<https://doi.org/10.1016/j.ijmactools.2009.08.002>. URL <https://www.sciencedirect.com/science/article/pii/S0890695509001667>
- [16] ASTM, [D6484-20: Standard test method for open-hole compressive strength of polymer matrix composite laminates \(2020\)](#). doi:[10.1520/D6484](https://doi.org/10.1520/D6484).
- [17] R. M'Saoubi, D. Axinte, S. L. Soo, C. Nobel, H. Attia, G. Kappmeyer, S. Engin, W.-M. Sim, [High performance cutting of advanced aerospace alloys and composite materials](#), *CIRP Annals* 64 (2) (2015) 557–580. doi:<https://doi.org/10.1016/j.cirp.2015.05.002>. URL <https://www.sciencedirect.com/science/article/pii/S0007850615001419>